Plasma diagnosis of tetrahedral amorphous carbon films by filtered cathodic vacuum arc deposition

Minglei WANG (王明磊)[1], **Lin ZHANG (张林)**[2,*], **Wenqi LU (陆文琪)**[1] **and Guoqiang LIN (林国强)**[1,*]

[1] Key Laboratory of Materials Modification by Laser, Ion, and Electron Beams of the Ministry of Education, Dalian University of Technology, Dalian 116024, People's Republic of China
[2] Key Laboratory of Green Fabrication and Surface Technology of Advanced Metal Materials of the Ministry of Education, Anhui University of Technology, Maanshan 243002, People's Republic of China

E-mail: wmllgq18@163.com

CrossMark

Abstract

Filtered cathodic vacuum arc (FCVA) deposition is regarded as an important technique for the synthesis of tetrahedral amorphous carbon (ta-C) films due to its high ionization rate, high deposition rate and effective filtration of macroparticles. Probing the plasma characteristics of arc discharge contributes to understanding the deposition mechanism of ta-C films on a microscopic level. This work focuses on the plasma diagnosis of an FCVA discharge using a Langmuir dual-probe system with a discrete Fourier transform smoothing method. During the ta-C film deposition, the arc current of graphite cathodes and deposition pressure vary from 30 to 90 A and from 0.3 to 0.9 Pa, respectively. The plasma density increases with arc current but decreases with pressure. The carbon plasma density generated by the arc discharge is around the order of 10^{10} cm^{-3}. The electron temperature varies in the range of 2–3.5 eV. As the number of cathodic arc sources and the current of the focused magnetic coil increase, the plasma density increases. The ratio of the intensity of the D-Raman peak and G-Raman peak (I_D/I_G) of the ta-C films increases with increasing plasma density, resulting in a decrease in film hardness. It is indicated that the mechanical properties of ta-C films depend not only on the ion energy but also on the carbon plasma density.

Keywords: filtered cathodic vacuum arc, Langmuir dual probe, plasma density, electron temperature

(Some figures may appear in colour only in the online journal)

1. Introduction

Amorphous carbon films are a kind of metastable material composed of sp^{2}C hybridization and sp^{3}C hybridization [1–5]. Recently, tetrahedral amorphous carbon (ta-C) film with a high sp^3 fraction has attracted increasing interest in various industrial fields due to its unique properties such as super hardness, excellent tribological behavior, chemical inertness, self-lubrication and surface adaptation [6–10].

Various deposition techniques such as magnetron sputtering, filtered cathodic vacuum arc (FCVA) deposition, ion beam assisted deposition and pulsed laser deposition have been employed for the synthesis of ta-C films [1, 7, 11, 12]. The FCVA method has the advantages of high incident particle energy, high ionization rate, and fast deposition rate [13, 14]. In particular, the production of ta-C films by arc discharge constitutes a classical example of plasma synthesis application in the field of vacuum science. Moreover, the microstructure and properties of ta-C films strongly depend on plasma parameters during cathodic vacuum arc discharge

* Authors to whom any correspondence should be addressed.

[15, 16]. To understand the formation mechanism of ta-C film and control the film growth, it is necessary to measure carbon plasma and precisely adjust ion flux [15, 17, 18].

The plasma diagnostic technique is fundamental for the deposition process of films by different plasma characterization methods, such as optical emission spectroscopy [19], quadrupole mass spectrometry [20, 21], retarding field energy analyzer [22] and Langmuir probe [15, 22–24]. Recently, the Langmuir probe method has been successfully applied to the measurement of plasma parameters, such as electron temperature, plasma density, and plasma space potential for the characterization of cathodic vacuum arc discharge in low-temperature plasmas and monitoring the process. However, due to the high density of carbon plasma in FCVA, the Langmuir single probe used commonly in the diagnosis of plasma parameters collects a large current in the region of electron saturation, resulting in red heat and even abnormal electron emission of the probe [25]. In addition, the carbon plasma generated by FCVA is very unstable, which makes the measured current–voltage (*I*–*V*) characteristic curve extremely unsmooth and difficult to directly use for plasma parameter analysis. To solve these problems, the Langmuir dual-probe system is designed, which exhibits obvious advantages compared to a single probe. The detected ion current is small and well below the ion saturation limit, so that it is protected from the influence of high-density arc plasma. For example, Thakur *et al* [26] reported that the current collected by the dual probe was 15–20 times smaller than that collected by a single probe, which facilitates diagnosis of plasma over a long period and avoids damaging the probe with too much current. Another is that the strong inherent fluctuation of the arc ion plating plasma is smoothed out using a discrete Fourier transform (DFT) algorithm. Moreover, the tip apex of the probe is designed in such a way that no deposition can result in a short circuit between the tip and its support [27]. Hence, the Langmuir dual-probe system, combined with the DFT smoothing method, is used to obtain the plasma average density and electron temperature. It can be considered an effective way to diagnose carbon plasma produced by FCVA.

In this study, the effects of the discharge arc current and the deposition pressure on the electron temperature and plasma density are investigated. The relationship between the number of arc sources and carbon plasma parameters is also studied. The plasma characteristics dependent on pressure, arc current and number of arc sources provide a further understanding of the deposition mechanism of ta-C films.

2. Experimental details

2.1. Langmuir probe measurements

To determine the carbon plasma characteristics such as plasma density and electron temperature during the synthesis of ta-C films, the Langmuir dual-probe system has been successfully developed in the laboratory. The probe system is the model of the MMLAB-prob series Langmuir probe system, based on the virtual instrument principle with the
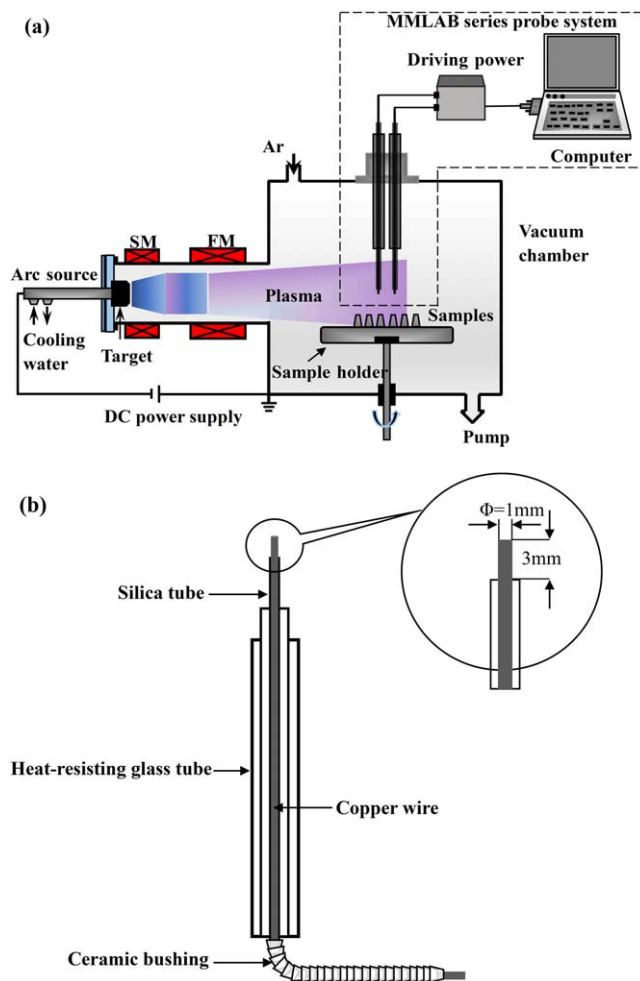

Figure 1. Schematic of the experimental setup (a) and structural diagram of the Langmuir probe (b).

advantages of simple structure, strong reliability and strong anti-disturbance ability. The Langmuir probe was mounted at the vacuum chamber of the FCVA system, as shown in figure 1(a). The site of probe diagnosis was located at the center of the chamber and the midline of the arc source. To filter macroparticles, the magnetic filter device has been designed as a system consisting of a source magnetic (SM) coil and a focused magnetic (FM) coil [28–30].

Figure 1(b) describes the structure of the Langmuir probe. The probe system is made of copper wire, ceramic bushing, a heat-resistant glass tube, a silica tube and probe needles composed of two cylindrical tungsten wires of 3 mm in length and 1 mm in diameter. The driving power connected with the probe was used to apply a sweeping voltage in the range of −50 to 50 V between the two probes. Plasma parameters of arc discharge in the vacuum chamber with a magnetic filter device were investigated, varying the working pressures from 0.3 to 0.9 Pa and the arc current of graphite cathodes from 30 to 90 A, respectively. The experiment details for plasma diagnosis are summarized in table 1.

The *I*–*V* curves were analyzed concerning the electron temperature T_e and the electron density n_e, as shown in figure 2. The curve of the saturated ion current region was
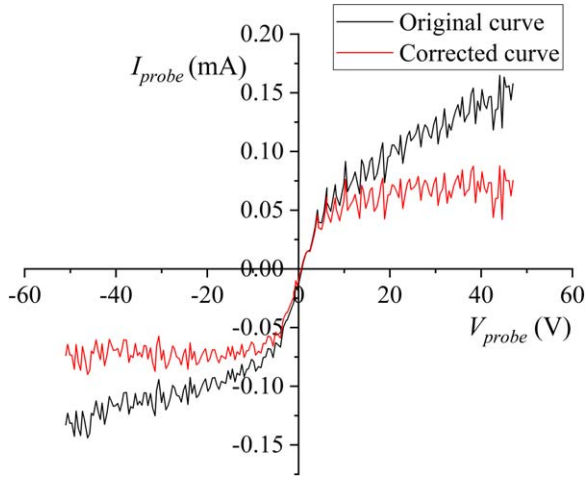
Figure 2. *I–V* curves.

Table 1. Langmuir probe experiment conditions.

Item	Value
Voltage range (V)	−50 to 50
Bias step (V)	0.50
Sampling rate (kS s^{-1})	125
Sampling number	500
Probe area (cm^2)	0.12
FFT factor	7
Gas pressure (Pa)	0.15–0.9
Arc current (A)	30–90

fitted linearly, and the saturated ion current was obtained from the intercept of the fitted line. The slope of the corrected curve can be used to calculate the electron temperature T_e, as shown in equation (1) [31].

$$T_e = \frac{e}{\kappa} \cdot \frac{dV}{d \ln I} \qquad (1)$$

where e is the electron charge and κ is the Boltzmann constant. The electron density n_e can be obtained using electron temperature T_e and saturated ion current $I_{i,sat}$, as confirmed in equation (2) [32].

$$n_e = \frac{I_{i,sat}}{e \cdot A} \cdot \sqrt{\frac{2\pi \cdot m_e}{\kappa \cdot T_e}} \qquad (2)$$

where $I_{i,sat}$ is the ion saturation current, m_e is the electron mass and A is the surface area of the probe.

2.2. Discrete Fourier transform smoothing method

If the function $f(x)$ represents the measured data $f(0), f(1), \ldots, f(2n-1)$, $f(x)$ can be expanded as a Fourier series:

$$f(x) \sim \frac{a_0}{2} + \sum_{k=1}^{N-1} \left[a_k \cos \frac{\pi}{N} kx + b_k \sin \frac{\pi}{N} kx \right] + \frac{a_N}{2} \cos \frac{\pi}{N} \pi x$$

where

$$a = \frac{1}{N} \sum_{m=1}^{2N-1} f(m),$$

$$a_N = \frac{1}{N} \sum_{m=1}^{2N-1} f(m) \cos m\pi,$$

$$a_k = \frac{1}{N} \sum_{m=1}^{2N-1} f(m) \cos \frac{\pi}{N} mk, \quad 1 \leqslant k \leqslant N-1,$$

$$b_k = \frac{1}{N} \sum_{m=1}^{2N-1} f(m) \sin \frac{\pi}{N} mk, \quad 1 \leqslant k \leqslant N-1.$$

$$f(x) = f_0(x) + N(x)$$

where $f_0(x)$ represents the inherent physical law of the measured data, and $N(x)$ represents the noise composition. If the function is smoother or more regularly periodic, the corresponding Fourier series converges faster. Since $f(x)$ is generally smooth and continuous, and noise $N(x)$ is essentially random and discontinuous, the convergence properties of their Fourier expansions are convergent and divergent, respectively. By truncating the Fourier series of $f(x)$ and discarding the high-frequency terms, the noise components can be greatly filtered and the measured curves become smoother.

2.3. Characterization of the deposited film

The bond structures of carbon atoms in the films were analyzed by a Raman spectroscope (Renishaw inVia, UK) using an Nd:He–Ne laser with a wavelength of 532 nm and an inverted microscope (ZEISS Axiovet model 25). The hardness and elastic modulus of the as-deposited films were characterized using a nano-indentation tester (MTS, 100BA-1C, USA). To avoid the influence of the substrate on the test results and ensure measurement accuracy, the indentation depth was controlled at about 140–160 nm and nine indentations were selected for each sample.

3. Results and discussion

In this work, the current of the FM coil is set as 0.25 A for magnetic type A and 0.5 A for magnetic type B. Meanwhile, the ratio of SM:FM is 2:1 for magnetic types A and B. The convergence effect of the carbon plasma increases at higher coil current of the focused magnetic field, as shown in figure 3(a). The combustion states of the target under magnetic fields A and B are divergent and convergent respectively.

Figure 3(b) displays the motion law of arc spots on the target's surface at different times for magnetic type B. The positive ions attracted to the cathode surface form a layer of space charge, which generates a strong electric field, and the cathode surface starts to emit electrons. Joule heating causes the temperature to rise to produce hot electrons, thereby further concentrating the current locally. At the same time, the ability of the cathode to emit electrons is closely related to the magnitude of its current. With increasing current, the
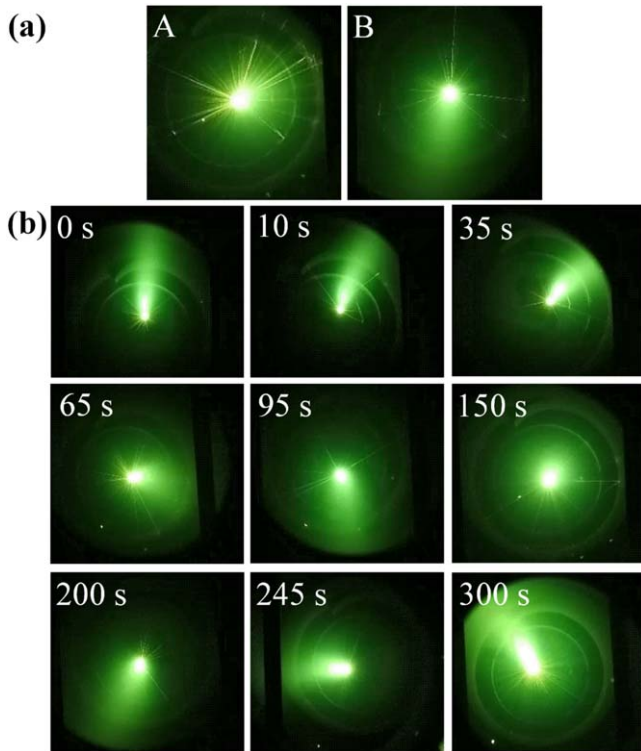
Figure 3. Arc discharge images of the graphite target. (a) Magnetic field-related discharge, (b) arc spot motion for magnetic type B.

Figure 4. Variation of plasma density as a function of magnetic type for arc current (a) and pressure (b).

emission of electrons increases, thus increasing the degree of ionization [33]. Subsequently, local ionization is generated on the cathode surface, emitting electrons and ions, and leaving discharge marks, which is also the process of arc spot formation. Therefore, the above process is repeated and the arc light spots move violently and irregularly on the cathode surface.

Figure 4 shows the plasma density as a function of the magnetic type. When the arc current is the same, the plasma densities for magnetic type B are higher than those for magnetic type A, as shown in figure 4(a). As an example of the arc current of 60 A, the plasma density is 1.80×10^{10} cm^{-3} and 2.69×10^{10} cm^{-3} for the magnetic types A and B, respectively. It is found from figure 4(b) that a similar phenomenon is observed in the case of working pressure, in which the plasma densities for magnetic type B are higher than those for magnetic type A. These results indicate that the plasma density increases with increasing coil current of the FM and the higher the current, the greater the focusing effect.

Figure 5 shows the effect of deposition parameters on the plasma density of a single target for magnetic field A. It is found that the plasma density increases gradually with increasing arc current from 30 to 90 A in figure 5(a). At the low pressure of 0.3 Pa, the plasma density is 0.29×10^{10} cm^{-3} for 30 A and 4.37×10^{10} cm^{-3} for 90 A, respectively. In the case of high pressure of 0.6 Pa and 0.9 Pa, the plasma density is approximately directly proportional to the arc current. The plasma density increases rapidly to 3.66×10^{10} cm^{-3} when the arc current is higher than 45 A, which could be attributed to carbon plasma disturbance generated by arc discharge of a

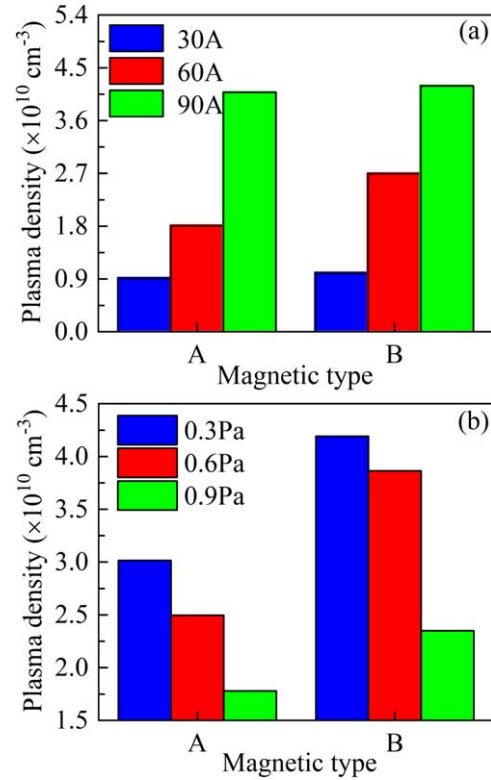single target at lower pressure. As shown in figure 5(b), plasma density decreases with increasing pressure at different arc currents. At low arc current, no obvious change is observed for 30 A and 45 A. However, it is quite distinct for higher arc currents above 60 A that the plasma density varies with the pressure. For the arc current of 90 A, the plasma density decreases from 4.37×10^{10} cm^{-3} at 0.3 Pa to 1.96×10^{10} cm^{-3} at 0.9 Pa with increasing pressure, which is attributed to collisions between ions, electrons, and neutral particles and reductions of ionic charges in the plasma. As the pressure increases, the mean free path of the electrons decreases, and the electrons gain less energy before colliding with the molecules, leading to fewer new electrons and ions [34]. In addition, the charges of ions in plasma decrease gradually with increases in deposition pressure and inelastic collision [34, 35]. Figure 5(c) presents the single target's electron temperatures as a function of the pressures at different arc currents. The electron temperature under a single target varies in the range of 2.06–3.42 eV. It can be seen that the electron temperature fluctuates greatly and without obvious regularity.

Figure 6 shows the effects of arc current and pressure on plasma characteristics under the double cathodic target discharge. Compared to the single target, the plasma density value generated by the double targets fluctuates much less. As the current increases from 30 to 90 A, the plasma density increases proportionally to the current, as shown in figure 6(a). Figure 6(b) shows the double targets' plasma density as a function of pressure from 0.3 to 0.9 Pa. Similar to
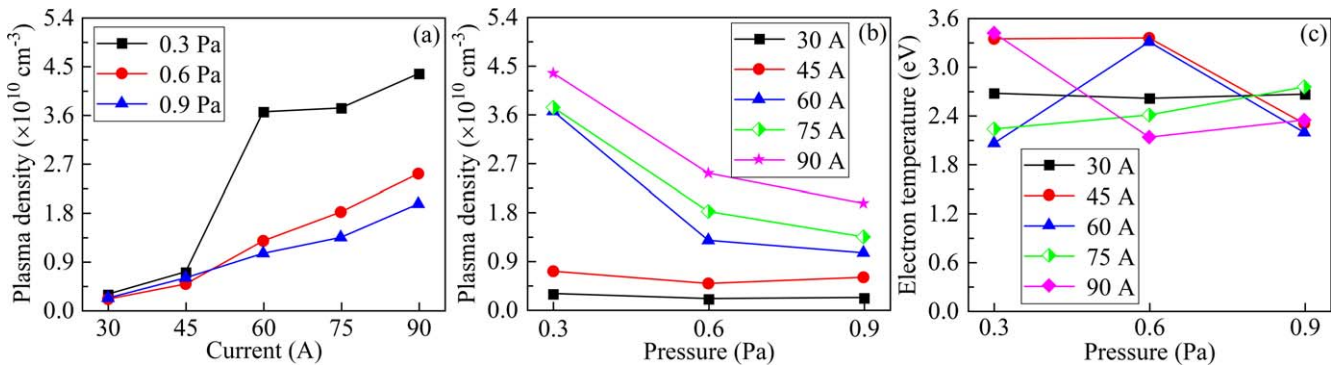
Figure 5. Variation of plasma density as a function of arc current (a) and pressure (b); variation of electron temperature (c) for the single target discharge.
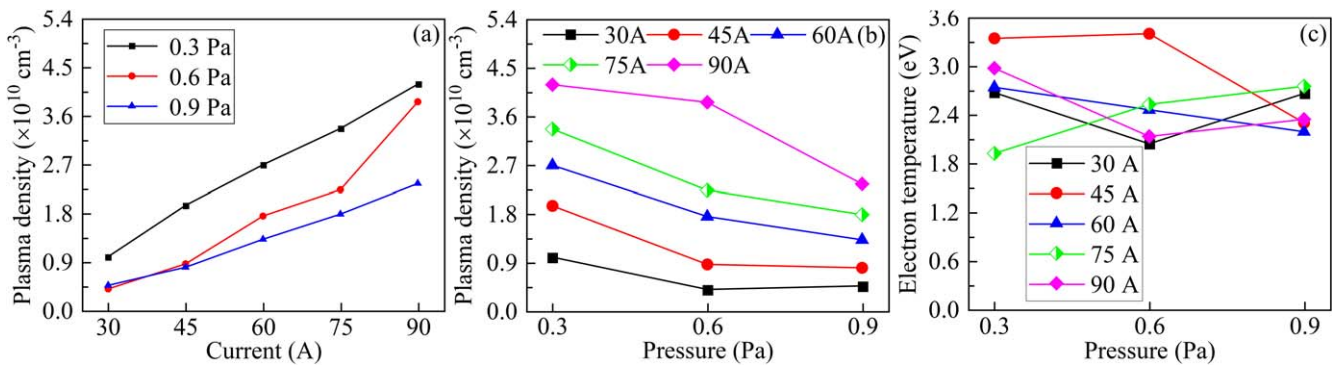

Figure 6. Variation of plasma density as a function of arc current (a) and pressure (b); variation of electron temperature (c) for the double target discharge.
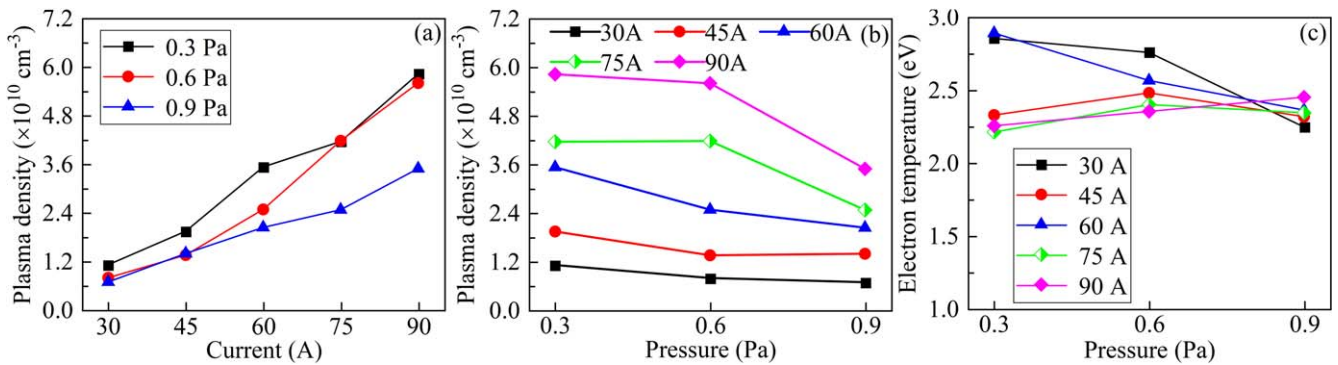

Figure 7. Variation of plasma density as a function of arc current (a) and pressure (b); variation of electron temperature (c) for three target discharge.

a single target, the plasma density under double targets decreases with increasing pressure gradually, and the change becomes more pronounced as the arc current increases. Figure 6(c) depicts the electron temperatures of the double targets. The electron temperatures of the double targets vary in the range of 1.92–3.41 eV.

Figure 7 exhibits the plasma characteristics measured under the three target discharge. The plasma density presents a similar trend to that of the single target and double targets. When the arc current changes from 30 to 90 A, the plasma density increases proportionally under the different pressures.

Like the single target and double targets, the plasma density decreases with increasing gas pressure gradually, as shown in figure 7(b). It is worth noting that the proportional relationship between plasma density and current is clearer for the three targets. Figure 7(c) shows the relationship between the electron temperatures and deposition pressure at the different discharge arc currents. Similar to the variation law of the single target and double targets, the electron temperature of three targets decreases with increasing gas pressure. It can be seen that when the pressure changes from 0.3 to 0.9 Pa, the electron temperature decreases from 2.89 to 2.22 eV. As the
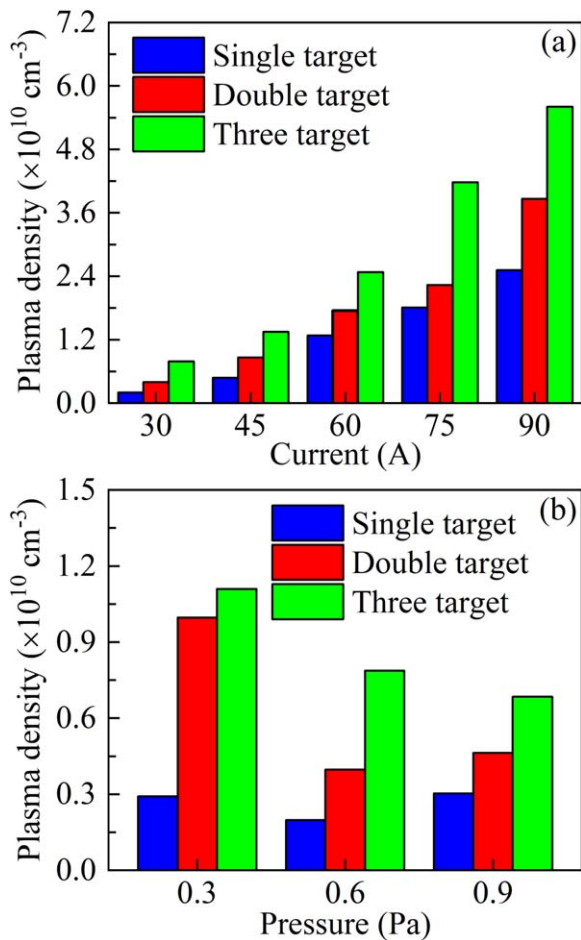
Figure 8. Variation of plasma density as a function of arc current (a) and pressure (b) for single target, double target, and three target discharge.
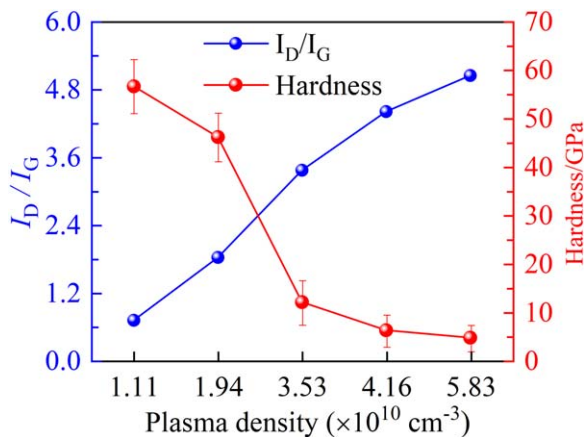

Figure 9. Ratio I_D/I_G and hardness of DLC films at different plasma densities.

gas pressure increases, the number of collisions per unit of time increases in the process of arc discharge, and kinetic energy exchange occurs between electrons and other particles, which leads to a decrease in electron temperature T_e. In addition, it is worth noting that compared with the single target and double targets, the fluctuation of electron

temperature of the three targets decreases with increasing gas pressure. This means that increasing gas pressure contributes to the continuity and stability of arc discharge.

Figure 8 illustrates the effects of arc current and gas pressure on the plasma density with different numbers of targets, respectively. It can be seen from figure 8(a) that when the arc current is constant, the plasma density increases with an increase in the number of targets in approximately direct proportion. Similar to figures 8(a) and (b) also shows the same variation of plasma density with the number of targets under the condition of constant pressure. In addition, compared with the single target and the double targets, the electron temperature fluctuations of the three targets are the smallest, indicating that the plasma tends to be stable at this time. Therefore, with the increase in the number of targets, the plasma becomes more and more stable and the electron temperature fluctuates less, which can provide a stable plasma environment for obtaining a more uniform film. It can be concluded that the arc current, gas pressure and number of target materials can have a direct impact on plasma characteristics.

To explain the relationship between the plasma parameters and film structure and properties, the carbon bonding structure and hardness of deposited ta-C films were characterized by Raman spectroscopy and the nano-indentation technique, respectively. The I_D/I_G ratio and hardness of as-deposited ta-C films are shown in figure 9. Generally, the fitted Raman spectra by Gaussian function can be divided into D-peaks around 1360 cm^{-1} and G-peaks around 1580 cm^{-1}. The D-peak is generated by the respiration vibration mode of the sp^2 atoms in the ring, and the G-peak is generated by the stretching motion of all pairs of sp^2 atoms in the ring or long chain [36, 37]. The intensity ratios of the D-peak to G-peak (I_D/I_G) can be employed to qualitatively analyze the fraction of sp^3 and sp^2 bonds in carbon films; that is, the smaller I_D/I_G, the higher the sp^3/sp^2 ratio. As the plasma density increases from 1.11×10^{10} to 5.83×10^{10} cm^{-3}, the I_D/I_G ratio increases from 0.71 to 5.05, while the hardness decreases from 56.67 to 4.69 GPa. This result indicates that the sp^3 bond fraction and hardness of DLC films decrease with the increase in plasma density. Based on the above results, the structure and mechanical properties of amorphous carbon films are closely related to plasma parameters.

It is well known from the subplantation model proposed by Lifshitz [38] and Robertson [39] that the properties of amorphous carbon film depend on the ion energy per C atom. The highest sp^3 bonding fractions are formed by C$^+$ ions with ion energy around 100 eV. When the ion energy is low, the ions cannot be injected into the sub-surface layer of the film, but just stick to the surface and grow in the way of sp^2 hybrid structure. When the ion energy is greater than 100 eV, the extra ion energy can cause local structure and stress relaxation of atoms inside the film, which promotes the transformation of some sp^3 hybrid bonds into sp^2 hybrid bonds, resulting in a decrease in the content of sp^3 hybrid bonds in the film. Therefore, in previous studies [40–42], it is generally accepted that the highest sp^3 fractions are formed by C$^+$ ions with ion energy around 100 eV. However, it can be concluded from this work

that the properties of ta-C films depend not only on the energy of ions but also on the value of plasma density. The carbon atoms that form ta-C films on the substrate are derived from carbon plasma, and the density of carbon plasma represents the number of carbon atoms in the plasma. Under the condition of low plasma density, the super-hard ta-C film can be obtained by FCVA, as shown in figure 9. With increasing plasma density, the carbon ions involved in the formation of sp^3 hybridization bond increase, and the excess ions cause coupling reaction with the formed sp^3 hybridization bonds and destroy sp^3 bonds to form more stable sp^2 hybridization bonds [43]. In addition, with increasing plasma density, the thermal peak effect is also induced, which makes the film structure relax and tend to sp^2 hybrid structure [44]. This is the reason why sp^3 hybridization bond in ta-C films decreases with an increase in plasma density. Hence, it can be concluded that the plasma characteristics during cathodic vacuum arc discharge play an important role in the microstructure and properties of ta-C films.

4. Conclusions

A Langmuir dual-probe system was established and successfully used to measure the carbon plasma parameters during the deposition process of ta-C films by an FCVA technique. The plasma characteristics of ta-C films were strongly affected by the deposition parameters including the focused magnetic field, arc current, pressure and number of cathodic targets. The plasma density increased proportionally with increasing coil current, arc current and number of cathodic targets, but decreased with increasing gas pressure. The electron temperatures varied in the range of 2–3.5 eV. The carbon plasma density generated by FCVA was of the order of 10^{-10} cm^{-3}, and directly influenced the microstructure and properties of the ta-C films. Ta-C films with super-hardness could be successfully deposited by adjusting the ion energy and carbon plasma density.

Acknowledgments

References

[1] Zarrabian M, Leteinturier C and Turban G 1998 *Plasma Sources Sci. Technol.* **7** 607
[2] Sun K and Diao D F 2020 *Carbon* **157** 113
[3] Kang Y F *et al* 2020 *Vacuum* **172** 109043
[4] Liu D P, Chen B X and Liu Y H 2006 *Plasma Sci. Technol.* **8** 285
[5] Wei J *et al* 2019 *Surf. Coat. Technol.* **374** 317
[6] Liao J *et al* 2004 *Carbon* **42** 387
[7] Zhou J *et al* 2006 *Plasma Sources Sci. Technol.* **15** 714
[8] Baby A *et al* 2011 *Plasma Sources Sci. Technol.* **20** 015004
[9] Argibay N *et al* 2018 *Carbon* **138** 61
[10] Zhang S *et al* 2019 *Carbon* **151** 136
[11] Obrosov A *et al* 2017 *Materials* **10** 156
[12] Bai L C *et al* 2011 *Nucl. Instrum. Methods Phys. Res.* **269** 1871
[13] Lin G Q *et al* 2009 *J. Vac. Sci. Technol.* **22** 1218
[14] Li H K, Lin G Q and Dong C 2009 *J. Vac. Sci. Technol.* **27** 1360
[15] Pang J H *et al* 2012 *Plasma Sci. Technol.* **14** 172
[16] Corbella C, Portal S and Zolotukhin D B 2019 *Plasma Sources Sci. Technol.* **28** 45016
[17] Shashurin A *et al* 2016 *Phys. Plasmas* **18** 073505
[18] Thakur G, Khanal R and Narayan B 2019 *Fusion Sci. Technol.* **75** 324
[19] Pastol A and Catherine Y 1990 *J. Phys. D: Appl. Phys.* **23** 799
[20] Bauer M, Schwarz-Selinger T and Jacob W 2005 *J. Appl. Phys.* **98** 073302
[21] Sugai H and Toyoda H 1992 *J. Vac. Sci. Technol.* **10** 1193
[22] Gahan D, Dolinaj B and Hopkins M B 2008 *Rev. Sci. Instrum.* **79** 033502
[23] Woodard A *et al* 2018 *Plasma Sources Sci. Technol.* **27** 104003
[24] Bai Y J *et al* 2016 *Plasma Sci. Technol.* **18** 58
[25] Pang J H *et al* 2012 *Plasma Sci. Technol.* **14** 172
[26] Thakur G, Khanal R and Narayan B 2019 *Fusion Sci. Technol.* **75** 324
[27] Ma X C *et al* 2018 *Plasma Sci. Technol.* **20** 025104
[28] Zhao Y H *et al* 2010 *J. Mater. Sci. Technol.* **26** 967
[29] Bäcker H and Bradley J W 2005 *Plasma Sources Sci. Technol.* **14** 419
[30] Li H K *et al* 2010 *Int. J. Refract. Met. Hard Mater.* **28** 544
[31] Andruczyk D *et al* 2006 *Plasma Sources Sci. Technol.* **15** 533
[32] Merlino R L 2007 *Am. J. Phys.* **75** 1078
[33] Zhao Y J *et al* 2022 *Plasma Sci. Technol.* **24** 055407
[34] Siegfried Z *et al* 2019 *J. Phys. D: Appl. Phys.* **52** 055201
[35] Zhirkov I *et al* 2015 *J. Appl. Phys.* **117** 213301
[36] Bootkul D *et al* 2014 *Appl. Surf. Sci.* **310** 284
[37] Sahu B B *et al* 2020 *J. Appl. Phys.* **127** 014901
[38] Lifshita Y *et al* 1990 *Phys. Rev.* **41** 10468
[39] Robertson J 1993 *Diam. Relat. Mater.* **2** 984
[40] Dong H *et al* 2019 *Surf. Coat. Technol.* **358** 987
[41] Zou Y S *et al* 2011 *Appl. Surf. Sci.* **258** 1624
[42] Zavaleyev V and Walkowicz J 2014 *Thin Solid Films* **581** 32
[43] Aijaz A and Kubart T 2017 *Appl. Phys. Lett.* **111** 051902
[44] Bai L C *et al* 2011 *Nucl. Instrum. Methods Phys. Res.* **269** 1871